Hypoxanthine Reduces Radiation Damage in Vascular Endothelial Cells and Mouse Skin by Enhancing ATP Production via the Salvage Pathway

Authors: Fujiwara, Megumi, Sato, Nana, and Okamoto, Ken

Source: Radiation Research, 197(6) : 583-593

Published By: Radiation Research Society

URL: https://doi.org/10.1667/RADE-21-00223.1

RADIATION RESEARCH **197**, 583–593 (2022)
0033-7587/22 $15.00

DOI: 10.1667/RADE-21-00223.1

Hypoxanthine Reduces Radiation Damage in Vascular Endothelial Cells and Mouse Skin by Enhancing ATP Production via the Salvage Pathway

Megumi Fujiwara,[a] Nana Sato[b] and Ken Okamoto[b,1]

[a] *Department of Biochemistry and Molecular Biology, Nippon Medical School, Tokyo, Japan; and* [b] *Department of Food Biotechnology and Structural Biology, Tokyo University, Tokyo, Japan*

Fujiwara M, Okamoto K, Sato N. Hypoxanthine Reduces Radiation Damage in Vascular Endothelial Cells and Mouse Skin by Enhancing ATP Production via the Salvage Pathway. *Radiat Res*. 197, 583–593 (2022).

An effective method that can protect radiation-damaged tissues from apoptosis and promote tissue repair has not been reported to date. Hypoxanthine (Hx) is an intermediate metabolite in the purine degradation system that serves as a substrate for ATP synthesis via the salvage pathway. In this study, we focused on the transient decrease in intracellular ATP concentration after radiation exposure and examined the protective effect of Hx against radiation-induced tissue damage. Human umbilical vein endothelial cells were X irradiated, and the cell viability and incidence of apoptosis and DNA double-strand breaks (DSBs) were evaluated at different Hx concentrations. We found that in the presence of 2–100 μM Hx, the percentages of DSBs and apoptotic cells after 2, 6 and 10 Gy dose of radiation significantly decreased, whereas cell viability increased in a concentration-dependent manner. Moreover, the addition of Hx increased the levels of AMP, ADP, and ATP in the cells at 2 h postirradiation, suggesting that Hx was used for adenine nucleotide synthesis through the salvage pathway. Administration of a xanthine oxidoreductase inhibitor to a mouse model of radiation dermatitis resulted in increased blood Hx levels that inhibited severe dermatitis and accelerated recovery. In conclusion, the findings provide evidence that increasing the levels of Hx to replenish ATP could be an effective strategy to reduce radiation-induced tissue damage and elucidating the detailed mechanisms underlying the protective effects of Hx could help develop new protective strategies against radiation.

INTRODUCTION

Radiation exposure can cause tissue damage. Recently, as seen in the case of the nuclear power plant accident caused by a major earthquake at the Fukushima Daiichi Nuclear Power Plant in Japan in March 2011, the risk of radiation exposure to employees of the facility and residents in the vicinity has been increasing. Against this background, the development of medical countermeasures against damages caused by radiation exposure has become increasingly important (*1*). In addition, radiation injury is a common complication of radiotherapy for cancer. Since skin and mucous membranes are susceptible to radiation damage, it is estimated that about 95% of patients with cancer undergoing radiation therapy will develop one of the following skin reactions: erythema, desquamation, dermatitis, ulceration, and fibrosis (*2*). These radiation-induced skin disease may limit the duration and dose of radiation therapy and lead to various complications, including increased risk of infection and decreased quality of life. However, there is still no treatment for radiation-induced tissue damage, and currently, only steroids and skin moisturizers are administered.

Upon exposure to radiation, a large amount of ATP is consumed in the process of protecting cells and repairing them during tissue damage, including radiation dermatitis. Particularly, after irradiation, intracellular ATP levels are markedly reduced (*3*), and increased energy demand in response to DNA damage affects the cellar repair process (*4*). Moreover, it has been reported that oral administration of adenosine and inosine, which are ATP precursors, resulted in survival and brain protection during total-body irradiation in mice (*5*). Therefore, it is expected that enhancing ATP synthesis could promote the repair of radiation-induced skin damage.

ATP is synthesized via two pathways that have different characteristics (*6, 7*). First is the *de novo* pathway, mainly involved in the synthesis of purines from amino acids and sugars. This pathway also synthesizes phosphoribosyl pyrophosphate, a component of ATP, and is preferentially activated in proliferating cells, such as lymphocytes (*8*). The other pathway, called the salvage pathway, recycles ATP

[1] Addresses for correspondence: Meguji Fujiwara, Ph.D., Department of Biochemistry and Molecular Biology, Nippon Medical School. 1-1-5 Sendagi, Bunkyo-ku, Tokyo 113-8602, Japan. mfujiwara@nms.ac.jp; and Ken Okamoto, Ph.D., Department of Food Biotechnology & Structural Biology, Tokyo University. 1-1-1 Yayoi, Bunkyo-ku, Tokyo 113-8657, Japan. akenokamoto@g.ecc.u-tokyo.ac.jp.

degradation products and uses hypoxanthine (Hx), an intermediary metabolite of ATP or GTP degradation, as a substrate for ATP synthesis (*9*). The major difference between the two pathways is the energy they require for ATP synthesis. The *de novo* pathway consumes five ATP molecules to synthesize one molecule of the inosine monophosphate (IMP) (*10*). In contrast, the salvage pathway does not consume ATP, making it more efficient (*11*). Moreover, the salvage pathways occur in tissues, such as the skeletal muscle, cardiac muscle, and neural tissue, which exhibit significant ATP consumption, and therefore, salvage pathways are thought to maintain ATP levels efficiently in these tissues (*6*, *12*). Therefore, it is expected that in pathological conditions where ATP is transiently and rapidly depleted, such as in radiation injury, promoting ATP synthesis through the salvage pathway might be useful for increased energy supply to avoid cell death due to irradiation damage.

Xanthine oxidoreductase (XOR) is an enzyme that produces uric acid using Hx and xanthine as substrates. XOR inhibition causes Hx accumulation that results in increased intracellular ATP synthesis via the salvage pathway, and this may contribute to the inhibition of tissue damage and the promotion of tissue repair (*13*, *14*). Based on this, a study found that XOR inhibitors could delay the pathological progression of amyotrophic lateral sclerosis in mice (*13*). XOR inhibitors have also been reported to protect the heart and kidney during ischemia-reperfusion injury (*14*, *15*). In addition, several studies have shown the significance of XO/XOR inhibitors in attenuating the effects of ionizing radiation. For example, one study has shown that radiation-induced endothelial dysfunction and cardiovascular complications can be effectively suppressed by inhibitors of XORs, which become more active and increase superoxide production in the liver and blood vessels after irradiation (*16, 17*). However, in this case, the effect of Hx, whose degradation is inhibited by XOR inhibitors and increases locally, has not been fully investigated.

The present study aimed to examine whether a direct or indirect increase in Hx can protect skin tissues against radiation damage and analyze the mechanism of this effect. Moreover, we examined the ability of Hx to reduce radiation damage and explored the role of Hx as a protective agent against radiation dermatitis.

MATERIALS AND METHODS

Cell Culture and Irradiation

Human umbilical vein endothelial cells (HUVECs; Takara Bio, Shiga, Japan) were grown in endothelial cell basal medium 2 (C-22011; Takara Bio) supplemented with growth factors and fetal bovine serum (FBS). All cells were cultured at 37°C under humidified conditions with 5% CO_2 as a general culture condition for 14 days. The medium was changed every other day, and cells with passage numbers of 6–7 were used for the experiments. X-ray irradiation experiments were performed at Nippon Medical School irradiation facility using a Hitachi MBR-1520R-3 device (150 kV, 20 mA, aluminum equivalent 0.5 mm, copper filter 0.1 mm, calculated dose rate 0.98 Gy/min). Cells were irradiated using 2, 6 and 10 Gy of X rays to evaluate cell viability, 6 and 10 Gy of X rays to evaluate apoptosis, and 6 Gy of X rays to evaluate the extent of DNA damage and changes in intracellular adenine nucleotide content. Immediately after irradiation, the HUVEC growth medium was replaced with a medium from which Hx was removed or a medium to which exogenous Hx was added.

Assessment of Cell Viability by WST-1 Assay and Cell Count

To evaluate the effect of Hx on cell viability after X irradiation, cell viability was examined using a Premix WST-1 Cell Proliferation Assay System (Takara, Shiga, Japan) according to the manufacturer's protocol. Briefly, HUVECs were seeded onto 96-well plates at a density of 1.5×10^3 cells/well and cultured in 200 μL medium for 24 h. When cells were 40–60% confluent, they were X irradiated and incubated at various concentrations of Hx in basal medium for 48 h. WST-1 reagent (10 μL) was added to each well and incubated for 3 h at 37°C. In this study, the WST-1 value was calculated according to the package insert of the measurement kit. In short, the WST-1 value was calculated by subtracting the absorbance of turbidity (630 nm) from the absorbance of the product, formazan (450 nm).

For the cell counting, cells were cultured as described in the *cell culture and irradiation* section. Subsequently, the cells were seeded onto 96-well plates at a density of 4,000 cells/well, and X irradiated as described above, after which the original medium was replaced with the medium from which Hx was removed or with the medium containing various concentrations of Hx and cultured for 48 h. The cells were then isolated by trypsin treatment, and the number of cells in each well was counted.

Culture with Superoxide Dismutase (SOD), Catalase and Uric Acid

SOD (5,000 U/mL), catalase (1,000 U/mL), or uric acid (2 μM) was added to the medium from which Hx was removed. Cell viability was measured using the WST-1 method as described above.

Terminal Deoxynucleotidyl Transferase-Mediated dUTP Nick-End Labeling (TUNEL) Assay

Cells were seeded at a density of 2×10^6 cells/chamber slides with or without Hx. After 24 h, 6 and 10 Gy X-irradiated cells were washed with phosphate-buffered saline (PBS) and fixed in 4% paraformaldehyde for 10 min at room temperature (~21–23°C). DNA fragmentation was performed using the Apoptosis in situ Detection Kit (Wako, Osaka, Japan). Apoptosis-positive cells appeared as brown-stained nuclei.

Comet Assay

The presence of DNA damage was assessed by single-cell electrophoresis using the OxiSelect Comet Assay Kit (Cell Biolabs, Inc., San Diego, CA) following the manufacturer's protocol. Cells were quantified using open-access ImageJ software (OpenComet) cell counter plugin. Approximately 300 cells per cell line per experiment were used for analysis.

Extraction of Purine Compounds and HPLC Analysis

Immediately after irradiation, the cell growth medium was replaced with Hx removed or added medium. After 2 h, the cell monolayer was washed twice with ice-cold PBS. Perchloric acid was added to the cells at a final concentration of 5%, and the mixture was centrifuged at 18,360 × g for 5 min to remove denatured proteins. The supernatant was transferred to a new tube, after which potassium carbonate was added at a final concentration of 0.6 M for neutralization. The mixture

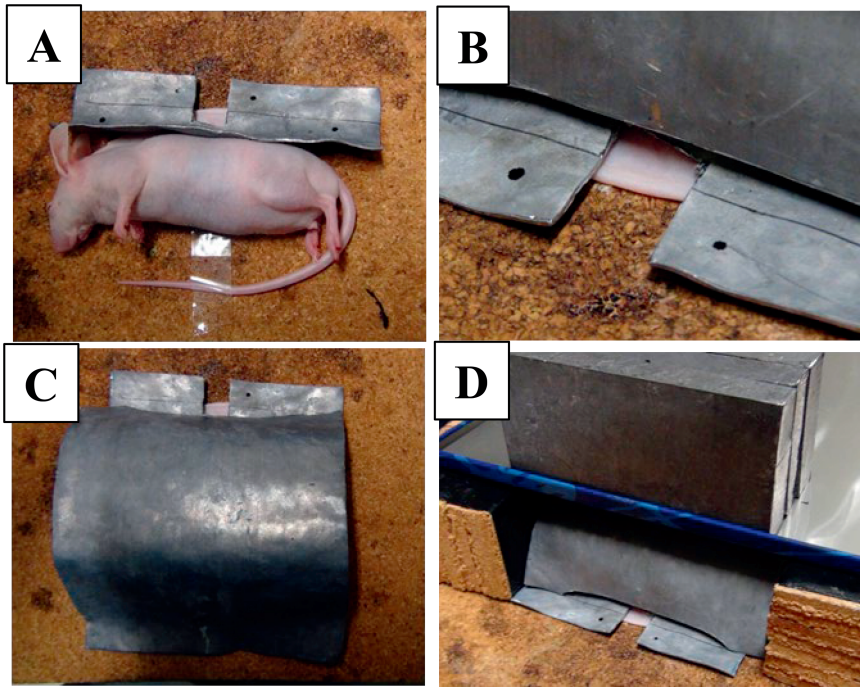

FIG. 1. Mouse (hairless) irradiation set-up. Panel A: Only the skin of the selected area was pulled out through the gap in the lead plate for irradiation. Panel B and C: All parts of the body were covered underneath the lead plate except for the selected part. Panel D: Several lead blocks were placed on top of the lead plates to shield the entire body from radiation.

was centrifuged at 18,360 × g for 5 min, and a quarter volume of 0.5 M potassium phosphate buffer (pH 5.5) was added to the supernatant.

Purine compounds in the cell extracts were quantified using a Shimadzu LC-20AD HPLC system (Shimadzu Corporation, Kyoto, Japan) with a SUPELCOSIL LC-18-T column (25 cm × 4.6 mm, 5-μm particle) connected to an LC-18-T Supelguard (2 cm × 4 mm, 5-μm particle). The analysis was performed at 40°C with a flow rate of 0.8 mL/min. The mobile phase and gradient program followed the method specified by Sigma Aldrich with a slight modification. The eluate was monitored at 254, 268, and 295 nm for the specific detection of Hx, xanthine, and uric acid, respectively. Adenine nucleotides were detected at a wavelength of 254 nm.

Calculation of Energy Charge

Energy charge (EC) is an indicator of the state of the intracellular adenine nucleotide pool and the normal metabolic regulation of ATP production and utilization systems (*18, 19*). And it is known that adenine nucleotides fluctuate to keep the energy charge as high as possible. Therefore, energy charge sensitively reflects abnormalities in energy metabolism in various pathological conditions (20). In this paper, the following equation was used to calculate the value of energy charge.

$$EC = (ATP + 1/2\ ADP)/(AMP + ADP + ATP).$$

Mice

Twenty-four normal hairless mice, (Hos:HR-1 mice 15 weeks old, male, 30.4–35.4 g in weight) were obtained from Sankyo Labo Service Corp. (Tokyo, Japan). The animals were housed under specific pathogen-free conditions. The animal room was controlled for temperature (22–24°C) and light (12-h light/dark cycles). All in vivo experimental protocols were approved by the Institutional Animal Care Committee of the Nippon Medical School (Approval No. 29-039).

Establishment and Evaluation of Radiation Dermatitis Model

Mice were distributed into two groups: 1. control group (Cont; n = 12) and 2. topiroxostat-treatment group (Topi; n = 12). Cont group mice were pre-fed with methylcellulose, whereas the Topi group mice were fed with 5 mg/kg topiroxostat 30 min before irradiation. For irradiation, the mouse's whole body was shielded using a dome-shaped lead plate except for a selected area of the animals' body. The skin of the selected area was pulled out of the slit in the lead plate and fixed with tape, the area (3 × 3 cm) was adjusted and exposed to the X rays (Fig. 1). The mice were then placed in the X ray machine (Hitachi MBR-1520R-3) under general anesthesia and X irradiated at 3.6 Gy/min until a total dose of 40 Gy was reached. After irradiation, the mice were returned to their original cages, and their body weights and measurements were recorded every other day for 28 d. Acute radiation dermatitis progresses from edematous erythema in mild cases to dry desquamation and exudative wet desquamation with increasing radiation dose (*21*). In this study, we evaluated the severity of the disease by calculating the area of wet desquamation, which is the most severe skin lesion among these symptoms, as a percentage of the irradiated area. Measurements were performed under anesthesia by tracing the irradiated area and area of wet desquamation following the method described in a previous study (*22*). The traced images were captured using Image J, and the ratio of the area of severe dermatitis to the total irradiated area was calculated.

Statistical Analyses

Results are presented as the mean ± SEM. One-way and two-way ANOVAs were used to analyze differences among groups, and Student's *t*-test was used to analyze the differences between two groups. A P value <0.05 was used to declare the statistical significance.

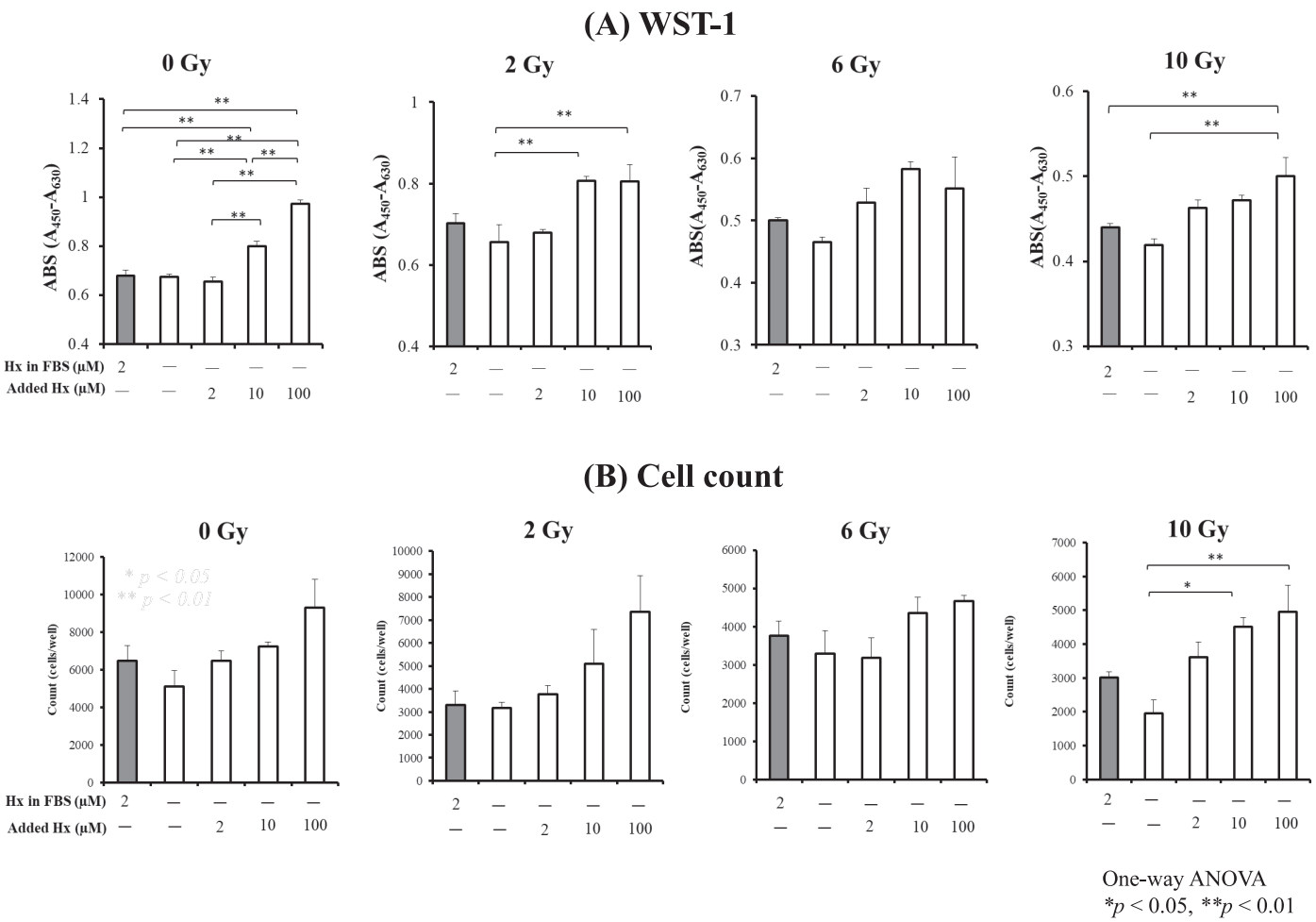

FIG. 2. The viability of human umbilical vein endothelial cells (HUVECs) at day 2 postirradiation to various X-ray doses. Immediately after irradiation, HUVECs, which were initially cultured in normal medium, were placed in hypoxanthine (Hx)-removed or added medium for 48 h. The WST-1 (A) and cell count methods (B) were used to assess differences in cell viability with and without Hx (n = 3 each). Gray bars represent cell viability in media containing endogenous Hx (2 μM), and white bars represent cell viability in media with endogenous Hx removed. The numbers under white bars indicate the final concentration of exogenous Hx added to media. For the WST-1 method, the value of the formazan product produced (450 nm) minus the value of the turbidity of the medium (630 nm) was plotted. Data are shown as mean ± SEM. $*P < 0.05$, $**P < 0.01$. Note that the scale of the Y-axis has been changed in the graph to get a clearer presentation.

RESULTS

Effect of Hx on the Viability of HUVECs after X Irradiation

FBS used for cell culture contained a high concentration of Hx at 110 μM. The final concentration of Hx in the standard medium containing FBS was estimated to be 2.2 μM, which was high enough to affect the experimental results; therefore, purified bovine XOR was added to remove Hx from the FBS before use. We confirmed that Hx in the FBS was no longer detected 16 h after the addition of XOR. We confirmed that XOR added to FBS loses its activity in the medium.

To evaluate the radioprotective effect of Hx on HUVECs, we examined whether the concentration of Hx in the medium altered the cell viability after irradiation. The results showed that even when the cells were not irradiated, cell proliferation was increased by the addition of Hx (10 μM and 100 μM; Fig. 2), whereas after 2, 6 and 10 Gy irradiation, the cell viability was decreased in a dose-dependent manner. On the contrary, after 2, 6, and 10 Gy irradiation, the protective effects of Hx were increased by 44.4%, 22.7% and 19.3%, respectively, in cells cultured with 100 μM Hx compared to cells grown in the medium without Hx. Further, at the same radiation doses, the effects increased by 43.3%, 14.5% and 13.6%, respectively, compared to cells grown on the normal medium containing 2 μM endogenous Hx. In this experiment, since Hx was added after X irradiation, our results suggest that the radioprotective effect of Hx was not because of its radical scavenging function but because of its effect on the repair mechanism of irradiated cells. The radioprotective effect of Hx plateaued at a concentration of 10 μM, and the same result was obtained by the cytometric method. In the cytometric assay, the addition of 10 μM Hx increased cell viability by 10–30 % compared to the cells cultured in the medium without Hx.

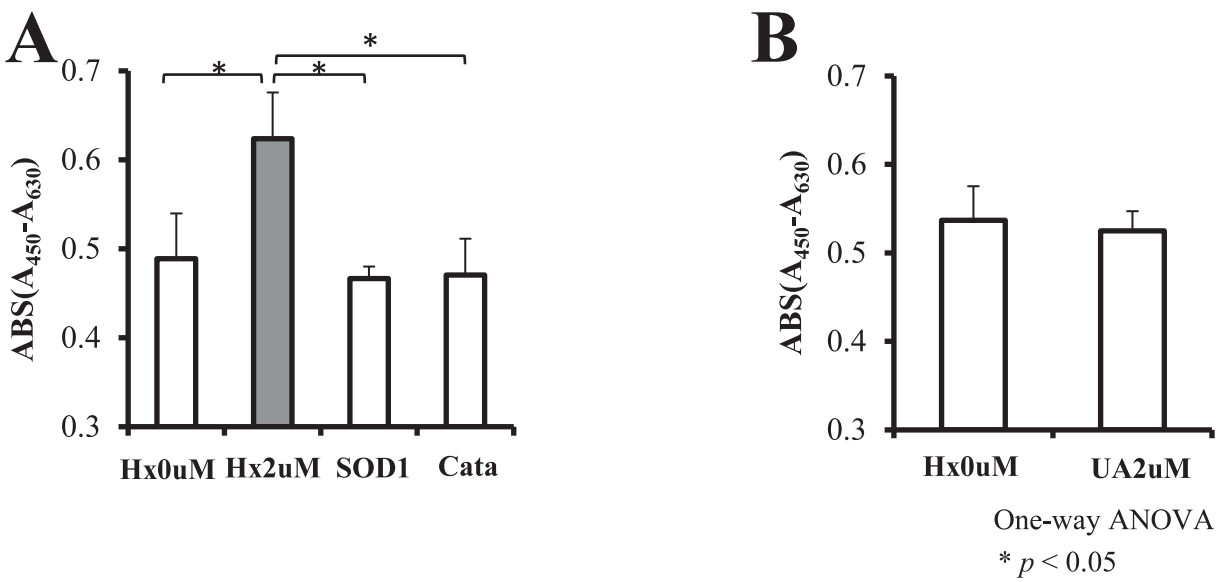

FIG. 3. Effects of H_2O_2, $O_2^{\bullet-}$, or uric acid on the radioprotection of cells. The cell viability was compared by adding (panel A) superoxide dismutase-1 (SOD; 5,000 U/mL), catalase (Cata; 1,000 U/mL), or (panel B) uric acid (UA; 2 μM) to the medium.

Effects of H_2O_2, $O_2^{\bullet-}$, or Uric Acid on the Radioprotection of Cells

To examine whether the oxidative stress caused by XOR-produced $O_2^{\bullet-}$ and H_2O_2 or the cytoprotective effect of XOR-produced uric acid would affect cell viability, purified XOR was added to remove Hx from the FBS-containing medium. Immediately after 2 Gy irradiation HUVECs, uric acid, SOD-1, catalase, or uric acid were added to HUVECs to evaluate whether they increased cell viability. The results showed that uric acid, $O_2^{\bullet-}$ or H_2O_2 did not increase cell viability (Fig. 3), confirming the radioprotective effect of Hx.

Effect of Hx on HUVEC Apoptosis after Irradiation

To evaluate the effect of Hx on postirradiation apoptosis in HUVECs, the TUNEL assay was performed. Hx concentrations were examined at 2 μM, which was sufficient to increase cell viability after irradiation, and at 100 μM, which was considered an excess dose. When Hx was removed from the medium immediately after irradiation, the percentage of TUNEL-positive cells at 24 h postirradiation increased fourfold compared to that in normal culture (Fig. 4), suggesting that Hx reduced postirradiation apoptosis in HUVECs. Therefore, we investigated the involvement of Hx in DSB repair, which can cause apoptosis. Using the comet assay, the extent of DNA damage 18 h postirradiation was assessed (*23*), with the tail length, tail DNA percentage, and tail moment as indicators of the degree of DNA damage. In the absence of Hx in the medium, tail length, tail DNA percentage, and tail moment at 18 h postirradiation increased by 2.7-, 2.7-, and 4.6-fold, respectively, compared with the values in the conventional medium (containing 2 μM Hx), indicating that there was increased radiation-induced DNA damage in the absence of Hx (Fig. 5). In addition, increasing the amount of Hx (from 2 μM to 100 μM) did not improve DNA damage suppression, suggesting that 2 μM of Hx was sufficient to protect DNA from fragmentation by 6 Gy irradiation.

Effects of Hx on the Amount of Adenine Nucleotides in HUVECs after Irradiation

To detect the changes in intracellular energy dynamics in the presence and absence of Hx postirradiation, we recorded the changes in intracellular adenine nucleotides. The results demonstrated the most significant decrease in intracellular ATP concentration at 2 h postirradiation (data not shown). Hence, we compared the intracellular ATP concentration in cells cultured in a medium with Hx removed or added, and the amount of adenine nucleotides per dish was measured at 2 h postirradiation. The results revealed increased intracellular ATP concentration after the addition of Hx (100 μM) compared to the removal of Hx (Fig. 6; $p < 0.01$). Hx increased the total adenine nucleotide content (ATP + ADP + AMP) with the increase of ATP, ADP and AMP. On the other hand, energy charge was 0.96 ± 0.003, 0.95 ± 0.005, and 0.95 ± 0.008 after irradiation in the Hx (0, 2, and 100 μM) groups, and did not change with the addition of Hx.

Confirmation of Increased Blood Hx Concentration by Topiroxostat Administration

A mouse model of skin irradiation damage was established to show that Hx exerts a radioprotective effect even in vivo. In contrast to that in cultured cells, Hx directly administered to mice was rapidly metabolized to allantoin (*24*). Accordingly, to increase the Hx levels in the blood, an XOR inhibitor was applied to the irradiation site. Indeed, we

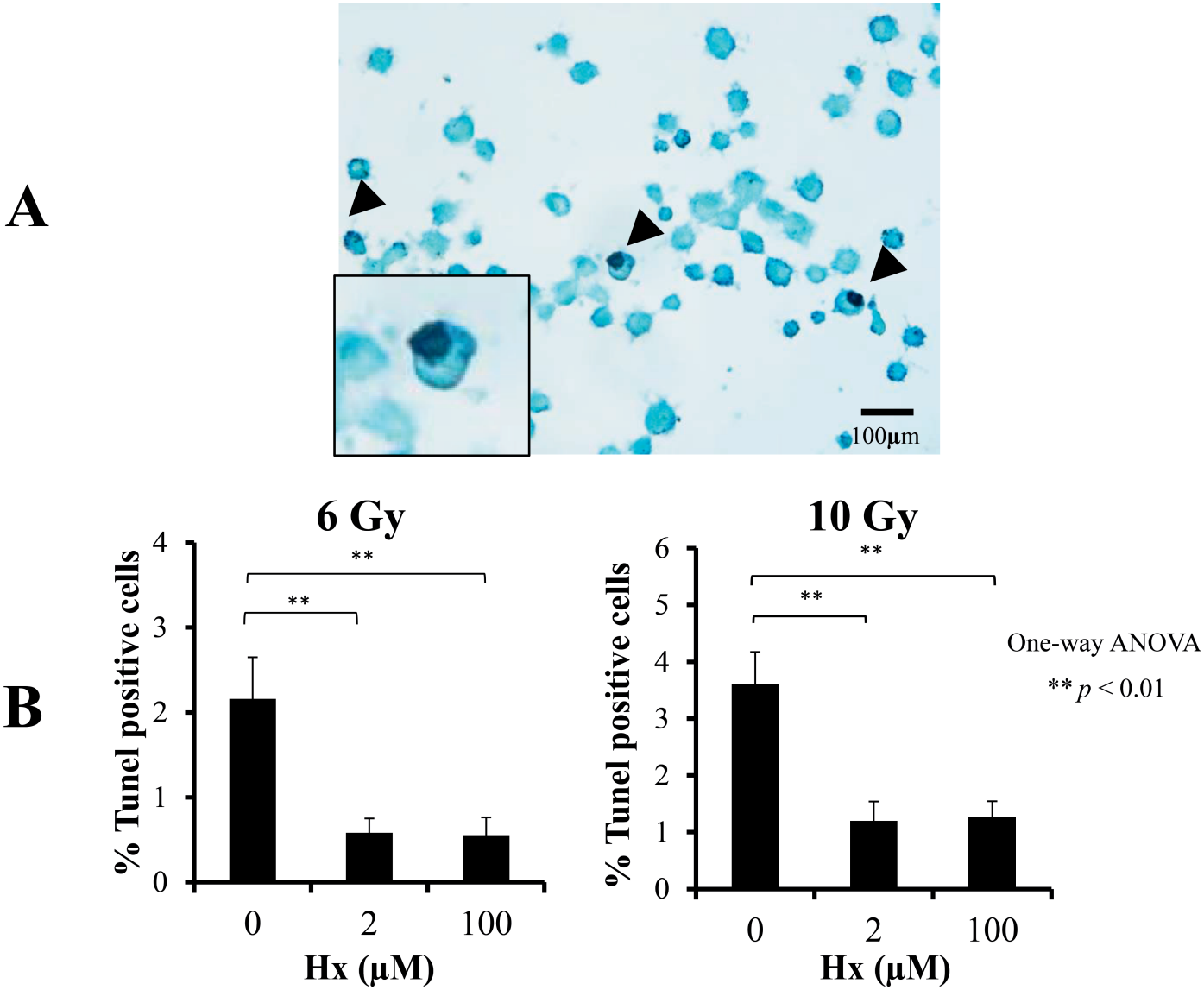

FIG. 4. Hypoxanthine (Hx) decreased apoptosis after either 6 or 10 Gy irradiation of human umbilical vein endothelial cells (HUVECs). Panel A: Apoptosis was assayed by terminal deoxynucleotidyl transferase dUTP nick end labeling (TUNEL) staining after a 10 Gy dose of radiation. Representative apoptotic cells are shown in the magnified inset. Arrowheads: apoptotic cells. Panel B: TUNEL-positive cells were quantified per field. When 2 μM Hx was added after irradiation, the percentage of TUNEL-positive cells at 24 h postirradiation was reduced to 25% of that in the normal medium.

observed a 6- and 12-fold increase in plasma Hx and xanthine concentrations, respectively, in mice at 1 h after topiroxostat administration (5 mg/kg, p.o.) (Fig. 7). At the same time, plasma uric acid levels decreased to 25% of control ($P < 0.05$). An increase in plasma Hx concentration from 2 μM to 12 μM was observed, and this concentration was sufficient to exert radioprotective effects at the cellular level, as shown in Fig. 2.

Irradiation Experiments on Mouse Skin

To evaluate whether such an increase in Hx has a protective effect on skin tissue, we administered topiroxostat to a mouse model of radiation dermatitis and evaluated the healing process of dermatitis. The set-up is shown in Fig. 1. There was no change in body weight throughout the observation period, even after irradiation, suggesting no systemic effects of radiation. The relative ratio of the area of severe dermatitis (moist desquamation) to the total irradiated area is plotted in Fig. 7.

In both the Topi and Cont groups, severe dermatitis began to form after 10 days, and the area of severe dermatitis peaked on day 14 postirradiation. Compared to the Cont group, the area of severe dermatitis in the Topi group was small from the beginning and remained small even on day 14 postirradiation, when severe dermatitis peaked. In the healing process after 14 days, the mice in the Topi group recovered more quickly (Fig. 7).

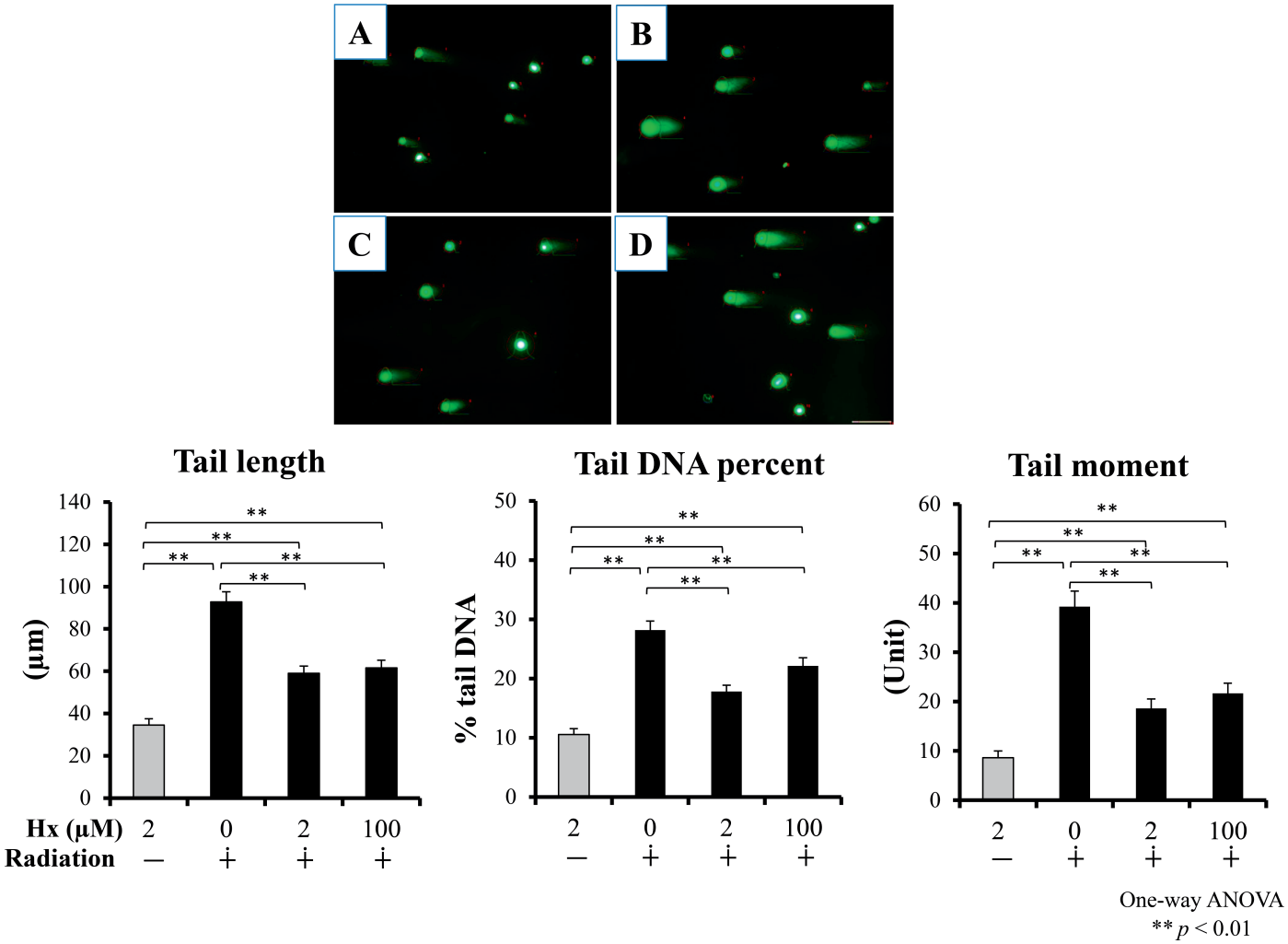

FIG. 5. Top panels: Photographs of the comet assay 18 h after 6 Gy irradiation. The red dots are artifacts in the analysis software. Panel A: unirradiated; panel B: 6 Gy irradiated and 0 μM hypoxanthine (Hx); panel C: 6 Gy irradiated and 2 μM Hx; and panel D: 6 Gy irradiated and 100 μM Hx. Bottom panels: Measurements of tail length, tail DNA percentages, and tail moments in the comet assay determined using the OpenComet software. Data are presented as mean ± SEM. At least 300 cells per sample and experiment were scored. $^{**}P < 0.01$.

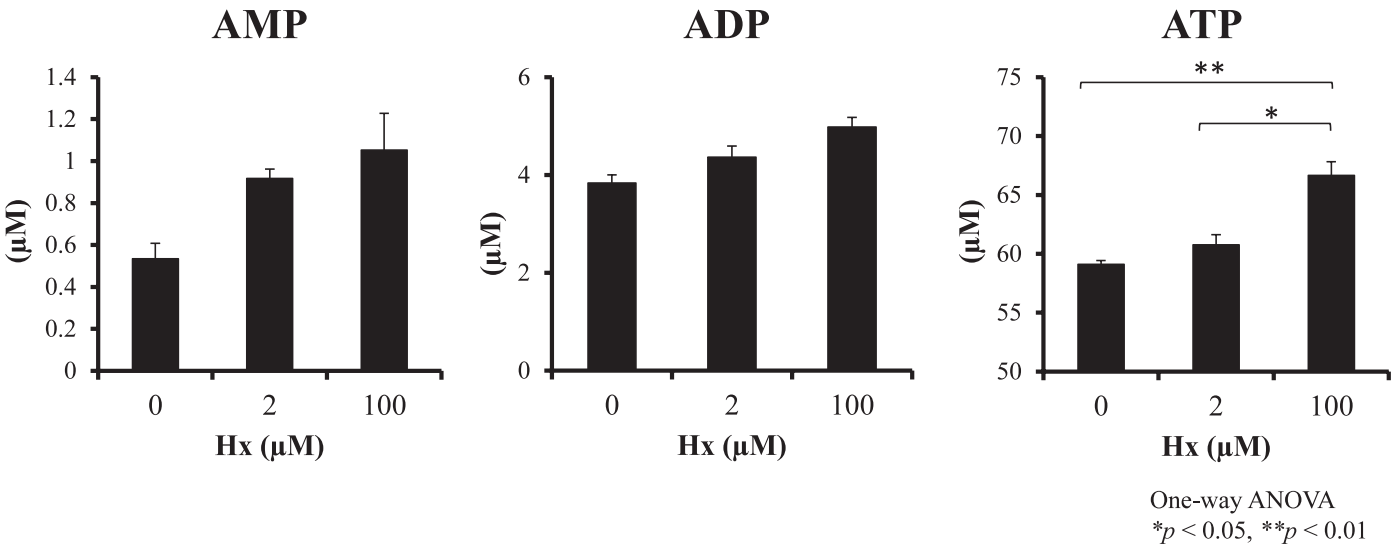

FIG. 6. Concentrations of adenine nucleotides (AMP, ADP and ATP) in human umbilical vein endothelial cells (HUVECs) at 2 h after 6 Gy irradiation. Concentrations are expressed as μmol/L per dish. Values are presented as mean ± SEM; n = 3, $^{*}P < 0.05$, $^{**}P < 0.01$.

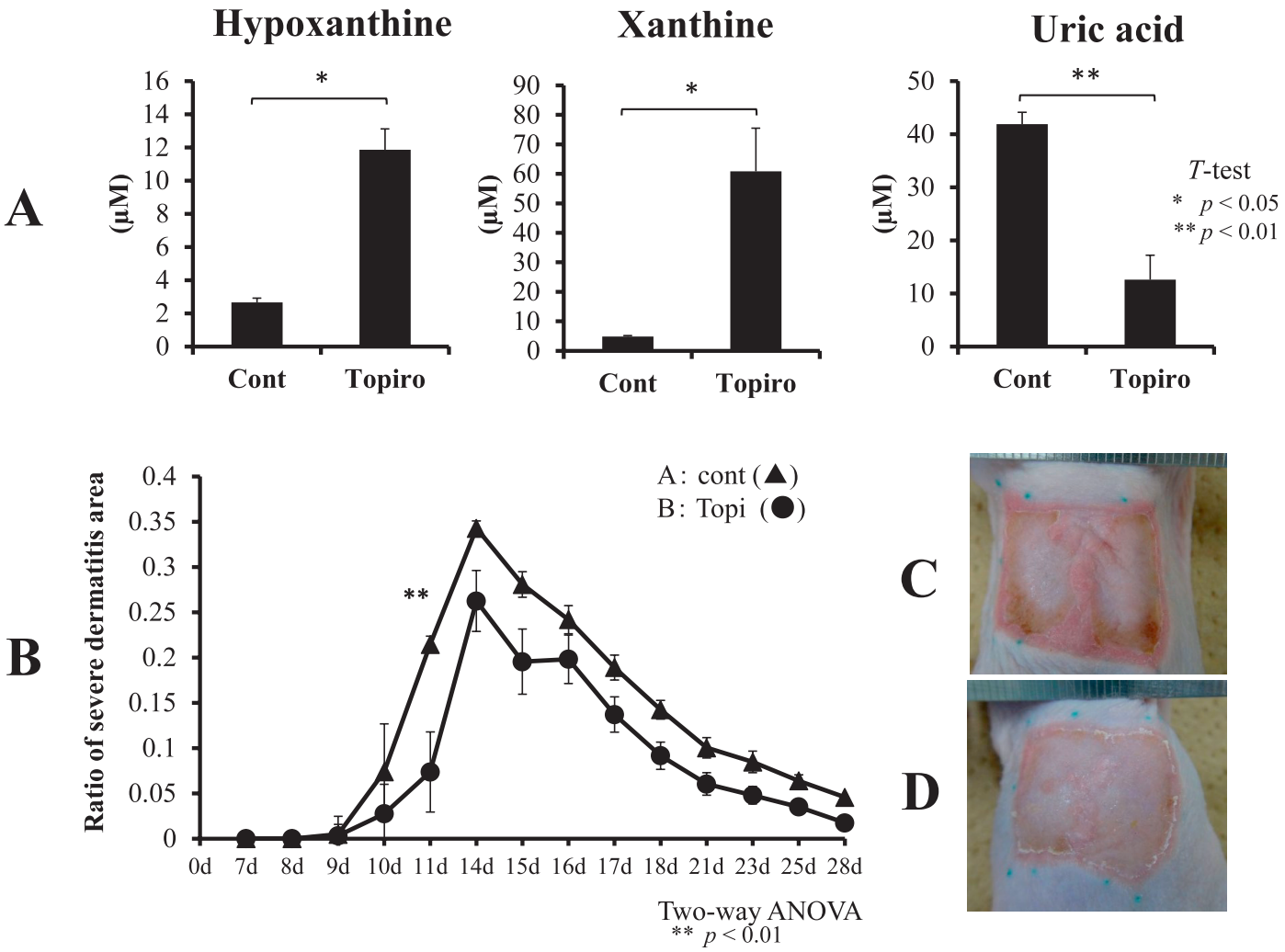

FIG. 7. Panel A: Blood hypoxanthine (Hx) and xanthine concentrations increased 1 h after administering the xanthine oxidoreductase (XOR) inhibitor, topiroxostat. Panel B: The relative ratio of the area of severe dermatitis (moist desquamation) to the total irradiated area from days 0–28 postirradiation in mice receiving methylcellulose or topiroxostat medication after a single 40 Gy dose of radiation. Representative photographs of mice in control (panel C) and topiroxostat-treated groups (panel D). $*P < 0.05$, $**P < 0.01$.

DISCUSSION

Radiation toxicity in normal tissues is an important issue in radiation-handling facilities, and it is one of the limiting factors in radiotherapy for patients with cancer. Reactive molecules, such as hydroxyl radicals, superoxide anions, hydrogen peroxide, and nitrogen dioxide, resulting from ionizing radiation, cause oxidative damage and cytotoxicity to cellular biomolecules. This causes a series of pathophysiological changes that lead to tissue damage, including apoptosis (*25*, *26*). At the cellular level, the intracellular ATP concentration decreases within a few hours after X irradiation and then eventually recovers (*3*). This change in intracellular energy metabolism is partly due to the temporary mitochondrial dysfunction caused by radiation, but it is most likely due to high ATP consumption during DNA repair after irradiation (*27*). The higher the dose, the more ATP is required for activating the protective mechanism. ATP in small intestinal tissues has been found to decrease 24 h after whole-body X-ray irradiation of minipigs, and the rate of decrease is significantly correlated with the severity of the pathology, suggesting that changes in energy metabolism contribute significantly toward the resulting radiological organ damage (*28*).

It is known that purine metabolism is an important determinant of tissue energy state because purine molecules form a part of high-energy phosphates, such as ATP and GTP. Under conditions of relalively increased ATP consumption, such as anaerobic conditions, ATP is degraded (*29–31*), and Hx produced as a degradation product is either converted to uric acid by XOR and excreted or partly used for ATP synthesis via the salvage pathway (*12*). The role of Hx in ATP synthesis is evident from several studies demonstrating that an increase in Hx in tissues can activate cells by increasing ATP synthesis via the salvage pathway (*32*, *33*). The present study demonstrated the cytoprotective (Fig. 2) and radioprotective (Fig. 3) effects of Hx. The energy charge, which indicates the

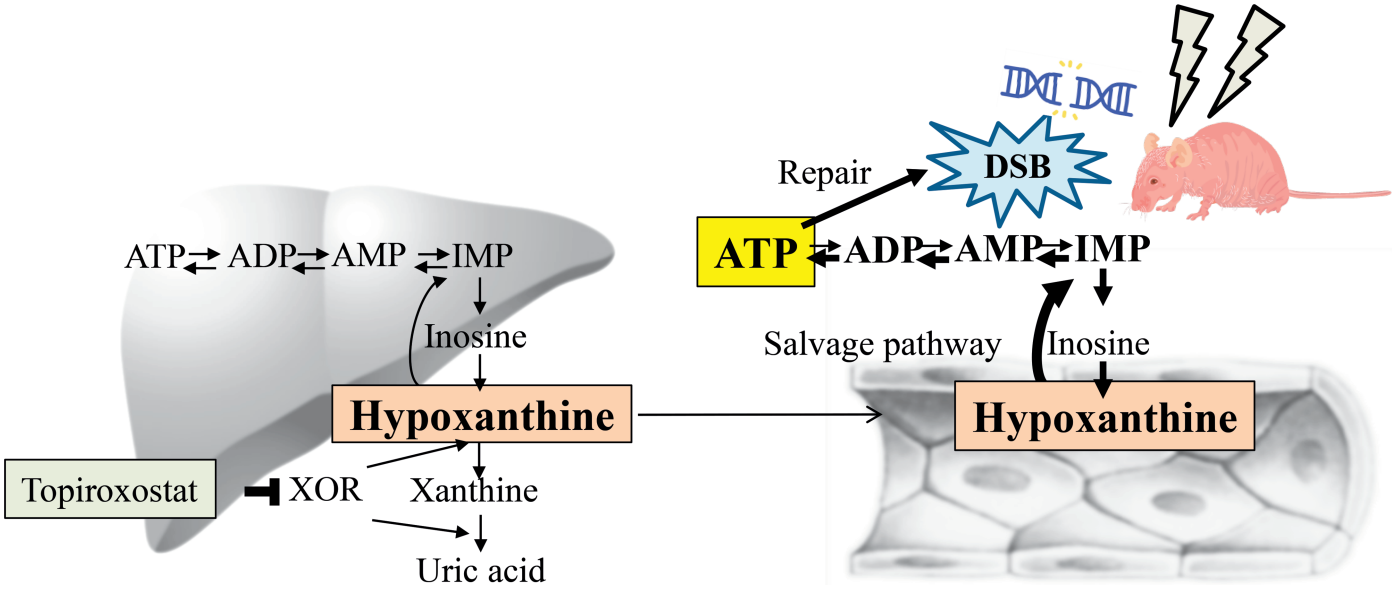

FIG. 8. Topiroxostat inhibits XOR, which are highly expressed in the liver, and causes the accumulation of hypoxanthine. When Hx increases in the liver, it is transported out of the liver by the bloodstream and reaches peripheral tissues such as the skin. As a result, transported Hx in the skin and other peripheral tissues can increase the resynthesis of intracellular ATP via the salvage pathway. On the other hand, the concentration of intracellular ATP is temporarily decreased upon exposure to radiation. Since a large amount of ATP is required to repair DNA double-strand breaks (DSBs), a decrease in ATP concentration leads to a delay in tissue repair. ATP enhancement by Hx can promote DNA repair and protect against radiation-induced skin damage.

balance between ATP synthesis and utilization systems, did not change after irradiation with or without Hx. This suggests that the degradation of adenine nucleotides was promoted to maintain the energy charge against the increase in ATP consumption in response to irradiation stress, and that the purine efflux from the cell was increased. In this situation, the addition of Hx was thought to increase the steady-state pool of total adenine nucleotides (ATP, ADP and AMP) in the cell via the salvage pathway, which could more easily meet the energy demand. Taken together, it can be inferred that replenishing ATP via increasing the accumulation of Hx could be an effective strategy to address radiation-induced organ damage.

In this study, we found that Hx increased the number of surviving cells after X irradiation, indicating its cytoprotective effect (Fig. 1). Hayashi et al. identified Hx as an important factor in the proliferation of porcine aortic endothelial cells. It has been reported that 14C-labeled Hx is incorporated into many purine metabolites, including ATP and GTP, and that Hx in the culture medium is taken up by the cells and utilized for ATP synthesis (*34*). The experimental results of this study support our result that the presence of Hx in the medium after irradiation increases ATP synthesis via the salvage pathway and improves cell viability.

Ionizing radiation can induce different types of DNA damage. The most toxic of which are DSBs that can be induced directly by high-energy ionizing radiation or indirectly by numerous toxic agents, leading to apoptosis if they cannot be repaired (*35*). An increase in postirradiation apoptosis is correlated with the extent of DNA damage resulting from DSBs generated during irradiation (*36–38*). In our results, Hx reduced the incidence of radiation-induced apoptosis and DSBs, suggesting that Hx might inhibit apoptosis associated with the generation of DSBs.

The repair process of damaged DNA requires a large amount of intracellular ATP (*27, 39–42*) and consists of the following steps: 1. alteration of chromatin structure by ATP-dependent chromatin remodeling factors, 2. recognition of DNA damage sites, and 3. processing of cleaved ends (DNA synthesis and linkage). In the first step, the damaged chromatin is removed from the DNA. At least six ATP-dependent chromatin remodeling factors use the hydrolytic energy of ATP to change the chromatin structure to expose the damaged DNA to repair factors (*43*), indicating. therefore, we hypothesized that Hx may promote DSB repair and decrease apoptosis by enhancing ATP synthesis. The present study also showed that the addition of Hx immediately after irradiation increased intracellular Hx and adeninenucleotide levels at 2 h postirradiation., suggesting that the increase in intracellular Hx concentration rescued ATP levels, which had decreased after irradiation, by utilizing Hx as a substrate for ATP synthesis via the salvage pathway. Collectively, it can be inferred that Hx could promote DSB repair and decrease apoptosis by enhancing ATP synthesis. Since our results indicate that Hx is beneficial for radioprotection, we assessed the effect of increased Hx concentration in the blood and tissues at the individual level. Direct oral administration of Hx is inappropriate for increasing blood Hx levels because it is quickly metabolized to allantoin in mice. Therefore, to increase the blood Hx concentration, an XOR inhibitor, which is also an anti-gout drug, was orally administered to

mice to stop purine degradation by Hx. It has been shown that XOR inhibitors increased intrahepatic and blood Hx levels by inhibiting XOR in the liver, which could be due to the fact that the catabolic metabolism of nucleic acids in vivo is mainly mediated by XOR, which is highly expressed in the liver. Reportedly, the administration of XOR inhibitors markedly increases blood Hx levels in mice and rats (*13,44*). Furthermore, it has also been shown that the administration of an XOR inhibitor (allopurinol) to patients with cancer before chemotherapy increased Hx levels by approximately 1.5-fold (*45*). Recently, increased levels of Hx in systemic tissues have been reported to activate local salvage pathways and help protect organs and prevent disease through increased ATP resynthesis (*14*). The role of XOR inhibitors to delay the disease progression by suppressing the formation of Bunina bodies in a mouse model of ALS through increased Hx levels and salvage activity in neurons has also been reported (*13*).

However, only a few studies have examined the effects of XOR inhibitors on radiation injury. The clinical effect of allopurinol rinses on the oral mucosa after radiation therapy is known to reduce the severity and frequency of mucositis (*46*, *47*). Inhibition of reactive oxygen species (ROS) production by XOR and the action of allopurinol as a radical scavenger have been proposed as mechanisms of action. In the present study, topiroxostat, a novel XOR inhibitor, reduced the area of severe dermatitis and the severity of radiation dermatitis. In a recent study, long-term observation of genetically modified mice expressing mutant XOR, which produces six times more ROS than mice expressing wild-type XOR, showed no obvious tissue damage caused by XOR-derived ROS (*48*). This study suggested that inhibiting XOR-derived ROS production did not have a significant effect and that the radioprotective effect of topiroxostat in this study was not due to inhibition of XOR-derived ROS production. Furthermore, topiroxostat, by itself, does not have chemical properties as a radical scavenger (*49*). Thus, the effect of topiroxostat is not from radical scavenging, but the effect of topiroxostat seems to be mediated by XOR inhibition. Therefore, it can be inferred that XOR inhibition by topiroxostat increased Hx levels and activated the salvage pathway, which increased ATP resynthesis and contributed to cell protection during irradiation. Based on these findings, we propose the following scheme describing the mechanism underlying the radioprotective effects of increased Hx levels (Fig. 8).

In conclusion, Hx increases the steady-state levels of ATP, ADP, and AMP after irradiation, thereby more readily meeting the energy demand after irradiation. As a result, Hx decreases the severity of radiation injury by increasing the survival of endothelial cells from DNA damage and apoptosis. The results were further validated in vivo using a mouse model of radiation dermatitis. However, one of the limitations of this study is that the nucleic acid metabolism is different between humans and mice; therefore, it is necessary to validate the results in humans in the future. The strategy of increasing blood Hx by Hx or anti-XOR inhibitors could be effective in preventing radiation dermatitis and mucositis during cancer treatment in humans and reducing exposure damage due to radiogenic accidents; however, it should be confirmed through further studies.

ACKNOWLEDGEMENTS

This study was supported by the Japan Society for the Promotion of Science (JSPS) KAKENHI (Grant Number: JP 18K15070) and by Fuji Yakuhin Co., Ltd.

Received: November 7, 2021; accepted: February 24, 2022; published online: March 25, 2022

REFERENCES

1. DiCarlo AL, Jackson IL, Shah JR, Czarniecki CW, Maidment BW, Williams JP. Development and licensure of medical countermeasures to treat lung damage resulting from a radiological or nuclear incident. Radiat Res. 2012; 177: 717–21.
2. Singh M, Alavi A, Wong R, Akita S. Radiodermatitis: a review of our current understanding. Am J Clin Dermatol. 2016; 17(3): 277–92.
3. Roy SJ, Koval OM, Sebag SC, Ait-Aissa K, Allen BG, Spitz DR, et al. Inhibition of CaMKII in mitochondria preserves endothelial barrier function after irradiation. Free Radic Biol Med. 2020; 146: 287–98.
4. Buranasudja V, Doskey CM, Gibson AR, Wagner BA, Du J, Gordon DJ, et al. Pharmacologic Ascorbate Primes Pancreatic Cancer Cells for Death by Rewiring Cellular Energetics and Inducing DNA Damage. Mol Cancer Res. 2019; 17(10): 2102-2114.
5. Gudkov SV, Gudkova OY, Chernikov AV, Bruskov VI. Protection of mice against X-ray injuries by the post-irradiation administration of guanosine and inosine. Int J Radiat Biol. 2009; 85(2): 116–25.
6. Ipata PL, Camici M, Micheli V, Tozz MG. Metabolic network of nucleosides in the brain. Curr Top Med Chem. 2011; 11(8): 909–22.
7. Moriwaki Y, Yamamoto T, Higashino K. Enzymes involved in purine metabolism – a review of histochemical localization and functional implications. Histol Histopathol. 1999; 14: 1321–40.
8. Federica M Marelli-Berg, Hongmei Fu, Claudio Mauro. Molecular mechanisms of metabolic reprogramming in proliferating cells: implications for T-cell-mediated immunity. Immunology. 2012; 136(4): 363–369.
9. Brown AK, Raeside DL, Bowditch J, Dow JW. Metabolism and salvage of adenine and hypoxanthine by myocytes isolated from mature rat heart. Biochim Biophys Acta. 1985; 845(3): 469-76.
10. Pedley AM, Benkovic SJ. A new view into the regulation of purine metabolism: The purinosome. Trends Biochem Sci. 2017; 42(2): 141–154.
11. Sculley DG, Dawson PA, Emmerson BT, Gordon RB. A review of the molecular basis of hypoxanthine-guanine phosphoribosyltransferase (HPRT) deficiency. Hum Genet. 1992; 90(3): 195–207.
12. Manfredi JP, Holmes EW. Purine salvage pathways in myocardium. Annu Rev Physiol. 1985; 47:691–705.
13. Kato S, Kato M, Kusano T, Nishino T. New strategy that delays progression of amyotrophic lateral sclerosis in G1H-G93A transgenic mice: oral administration of xanthine oxidoreductase inhibitors that are not substrates for the purine salvage pathway. J Neuropathol Exp Neurol. 2016; 75(12): 1124–44.
14. Johnson TA, Jinnah HA, Kamatani N. Shortage of cellular ATP as a cause of diseases and strategies to enhance ATP. Front Pharmacol. 2019; 10: 98.

15. Tani T, Okamoto K, Fujiwara M, Katayama A, Tsuruoka S. Metabolomics analysis elucidates unique influences on purine/pyrimidine metabolism by xanthine oxidoreductase inhibitors in a rat model of renal ischemia-reperfusion injury. Mol Med. 2019; 25(1): 40.
16. Srivastava M, Chandra D, Kale RK. Modulation of radiation-induced changes in the xanthine oxidoreductase system in the livers of mice by its inhibitors. Radiat Res. 2002; 157(3): 290-7.
17. Soucy KG, Lim HK, Attarzadeh DO, Santhanam L, Kim JH, Bhunia AK et al. Dietary inhibition of xanthine oxidase attenuates radiation-induced endothelial dysfunction in rat aorta. J Appl Physiol. 1985. 2010; 108(5): 1250-8.
18. Atkinson DE, Walton GM. Adenosine triphosphate conservation in metabolic regulation. Rat liver citrate cleavage enzyme. J Biol Chem. 1967; 242(13): 3239-41.
19. Atkinson DE. The energy charge of the adenylate pool as a regulatory parameter. Interaction with feedback modifiers. Biochemistry. 1968; 7(11): 4030-4.
20. Uetaki M, Tabata S, Nakasuka F, Soga T, Tomita M. Metabolomic alterations in human cancer cells by vitamin C-induced oxidative stress Sci Rep. 2015; 5: 13896.
21. Singh M, Alavi A, Wong R, Akita S. Radiodermatitis: A review of our current understanding. Am J Clin Dermatol. 2016; 17(3): 277-92.
22. Korpela E, Yohan D, Chin LC, Kim A, Huang X, Sade S, et al. Vasculotide, an Angiopoietin-1 mimetic, reduces acute skin ionizing radiation damage in a preclinical mouse model. BMC Cancer. 2014; 14: 614.
23. Olive PL, Banáth JP. Sizing highly fragmented DNA in individual apoptotic cells using the comet assay and a DNA crosslinking agent. Exp Cell Res. 1995; 221(1): 19-26.
24. Moyer JD, Henderson JF. Salvage of circulating hypoxanthine by tissues of the mouse. Can J Biochem Cell Biol. 1983; 61: 1153-7.
25. Leach JK, Van Tuyle G, Lin PS, Schmidt-Ullrich R, Mikkelsen RB. Ionizing radiation-induced, mitochondria-dependent generation of reactive oxygen/nitrogen. Cancer Res. 2001; 61: 3894–901.
26. Spitz DR, Azzam EI, Li JJ, Gius D. Metabolic oxidation/reduction reactions and cellular responses to ionizing radiation: a unifying concept in stress response biology. Cancer Metastasis Rev. 2004; 23(3-4): 311–22.
27. Qin L, Fan M, Candas D, Jiang G, Papadopoulos S, Tian L, et al. CDK1 enhances mitochondrial bioenergetics for radiation-induced DNA Repair. Cell Rep. 2015; 13(10): 2056–63.
28. Wang YJ, Liu W, Chen C, Yan LM, Song J, Guo KY, et al. Irradiation induced injury reduces energy metabolism in small intestine of Tibet minipigs. PLoS One. 2013; 8(3): e58970.
29. Weiner MW. NMR spectroscopy for clinical medicine. Animal models and clinical examples. Ann N Y Acad Sci. 1987; 508: 287–99.
30. Lasley RD, Ely SW, Berne RM, Mentzer Jr RM. Allopurinol enhanced adenine nucleotide repletion after myocardial ischemia in the isolated rat heart. J Clin Invest. 1988; 81(1): 16–20.
31. Stromski ME, van Waarde A, Avison MJ, Thulin G, Gaudio KM, Kashgarian M, et al. Metabolic and functional consequences of inhibiting adenosine deaminase during renal ischemia in rats. J Clin Invest. 1988; 82(5): 1694–9.
32. Mink R, Johnston J. The effect of infusing hypoxanthine or xanthine on hypoxic-ischemic brain injury in rabbits. Brain Res. 2007; 1147: 256–64.
33. Hayashi Y, Hirai S, Harayama H, Saito T, Ichikawa A. Identification of hypoxanthine and inosine in brain dialyzable fraction as stimulators for growth of porcine aortic endothelial cells in response to fibroblast growth factor in either dialyzed serum media or low serum media. Jpn J Pharmacol. 1990; 53(1): 1–9.
34. Hirai S, Hayashi Y, Koizumi T, Nakanishi N, Fukui T, Ichikawa A. Fibroblast growth factor-dependent metabolism of hypoxanthine via the salvage pathway for purine synthesis in porcine aortic endothelial cells. Biochem Pharmacol. 1993; 45(8): 1695–701.
35. Roos WP, Kaina B. DNA damage-induced cell death: from specific DNA lesions to the DNA damage response and apoptosis. Cancer Lett. 2013; 332(2): 237–48.
36. Whitaker SJ, Ung YC McMillan TJ. DNA double-strand break induction and rejoining as determinants of human tumour cell radiosensitivity. A pulsed-field gel electrophoresis study. Int J Radiat Biol. 1995; 67: 7–18.
37. Wurm R, Burnet NG, Duggal N, Yarnold JR, Peacock JH. Cellular radiosensitivity and DNA damage in primary human fibroblasts. Int J Radiat Oncol Biol Phys. 1994; 30: 625–33.
38. Lips J, Kaina B. DNA double-strand breaks trigger apoptosis in p53-deficient fibroblasts. Carcinogenesis. 2001; 22(4): 579–85.
39. Maruta H, Matsumura N, Tanuma S. Role of (ADP-ribose)n catabolism in DNA repair. Biochem Biophys Res Commun. 1997; 236: 265–69.
40. Friedman DL, Mueller GC. A nuclear system for DNA replication from synchronized HeLa cells. Biochim Biophys Acta. 1968; 161: 455–68.
41. Lynch WE, Brown RF, Umeda T, Langreth SG, Lieberman I. Synthesis of deoxyribonucleic acid by isolated liver nuclei. J Biol Chem. 1970; 245: 3911–16.
42. Krokan H, Bjorklid E, Prydz H. DNA synthesis in isolated HeLa cell nuclei. Optimization of the system and characterization of the product. Biochemistry. 1975; 14: 4227–32.
43. Osley MA, Tsukuda T, Nickoloff JA. ATP-dependent chromatin remodeling factors and DNA damage repair. Mutat Res. 2007; 618(1-2): 65–80.
44. Szasz T, Davis RP, Garver HS, Burnett RJ, Fink GD, Watts SW. Long-term inhibition of xanthine oxidase by febuxostat does not decrease blood pressure in deoxycorticosterone acetate (DOCA)-salt hypertensive rats. PLoS One. 2013; 8: e56046.
45. Wung WE, Howell SB. Hypoxanthine concentrations in normal subjects and patients with solid tumors and leukemia. Cancer Res. 1984; 44(7): 3144–8.
46. Worthington HV, Clarkson JE, Eden OB. Interventions for treating oral mucositis for patients with cancer receiving treatment. Cochrane Database Syst Rev. 2004; (2): CD001973.
47. Yasuda T, Chiba H, Satomi T, Matsuo A, Kaneko T, Chikazu D, et al. Preventive effect of rebamipide gargle on chemoradiotherapy-induced oral mucositis in patients with oral cancer: a pilot study. J Oral Maxillofac Res. 2012; 2(4): e3.
48. Ali MR, Kumar S, Afzal O, Shalmali N, Ali W, Sharma M et al. 2-Benzamido-4-methylthiazole-5-carboxylic Acid Derivatives as Potential Xanthine Oxidase Inhibitors and Free Radical Scavengers. Arch Pharm (Weinheim). 2017; 350(2). 10.
49. Kusano T, Ehirchiou D, Matsumura T, Chobaz V, Nasi S, Castelblanco M, et al. Targeted knock-in mice expressing the oxidase-fixed form of xanthine oxidoreductase favor tumor growth. Nat Commun. 2019; 10(1): 4904.